Pergamon

Journal of Structural Geology, Vol. 16, No. 3, pp. 303 to 313, 1994
Elsevier Science Ltd
Printed in Great Britain
0191-8141/94 $06.00+0.00

Flow and deformation of viscous, silica-oversaturated dispersions in low-grade faults

H. STEL and A. C. LANKREYER

Institute of Earth Sciences, Vrije Universiteit Amsterdam, de Boelelaan 1085, 1081 HV Amsterdam, The Netherlands

(*Received* 13 *July* 1992; *accepted in revised form* 6 *May* 1993)

Abstract—Cryptocrystalline silica veins occur along shear faults and in dilatational cracks in low-grade cataclasites derived from leucocratic granitoids. The silica minerals occur as radiate bladed quartz, and as spherulitic and sheaf-like clusters of neocrystallites that nucleated on crush fragments in a matrix of opaline and chalcedony. This texture is indicative of rapid crystallization from a viscous, oversaturated fluid. The veins are clast-loaded, and typically demonstrate a banding defined by variation in the amount and size of feldspar crush fragments. Three types of veins are distinguished that differ in relative timing of viscous fluid flow, deformation and crystallization. Type (1) veins are dilatational cracks, in which static settling and crystallization took place. An undisturbed, planar layering is found, which has no fixed orientation with respect to the vein wall. This banding is commonly associated with a layering defined by periodic variations in hematite precipitates. Type (2) veins show a gradual decrease in grain size of the crush fragments from one vein wall to the other. This banding shows pinch-and-swell structures, micro boudinage and folding, suggestive of flow. Type (3) veins occur in shear faults and demonstrate a banding which is asymmetric with respect to the vein walls. Apart from pinch-and-swell structures and folds, the foliation shows sigmoidal deflection similar to that in shear bands in ductile mylonites. It is proposed that the cryptocrystalline, fragment loaded veins are formed by solidification of a silica sol or hydrogel that was formed by quenching of a hot, fragment-bearing solution during brittle failure. The effect of a viscous fluid in fault rock is discussed in terms of rheology and of seismic periodicity.

INTRODUCTION

FAULT gouge is an extremely fine-grained 'smear' that occurs along a brittle fault and is composed of crush fragments, neocrystalline phases, hydrothermally altered minerals and amorphous material. Gouge is generally a ductile substance, and may accommodate non-seismic slip by its lubricating effect on cataclastic flow (Engelder *et al.* 1975, Rutter & White 1979, Dieterich & Conrad 1984, Rutter *et al.* 1986, Yund *et al.* 1990, Chester *et al.* 1993). Flow behaviour of gouge determines the rheology of fault zones and in this way it may locally govern the state of stress in faulted crust (Zoback *et al.* 1987). The study of fault gouge is therefore one of the main topics in current experimental and observational research on fault rocks (Babaie *et al.* 1991, Chester & Higgs 1992, Rutter & Maddock 1992). In an earlier paper, one of us (Stel 1981) suggested that neocrystalline silica in low-grade cataclasites originated from solidification of silica gel. This idea was based on the strong similarity of the microstructure of cryptocrystalline silica minerals in cataclasites with the textures of experimentally crystallized silica gels (Oehler 1976). However, at the time no indications were found of its relative age with respect to deformation in the fault, as no microstructures were found from which the flow behaviour of the supposed gel could be deduced. Moreover, no good model was available to explain the formation of a gel phase during cataclasis. In this paper we report new evidence for a syn-kinematic presence of a viscous, silica oversaturated fluid in fault zones. Apparently paradoxical microstructures are observed in fault gouge when studied on different scales. On a micrometre scale undeformed crystallites are found, which display textures indicative of rapid crystallization. On the millimetre to centimetre scale, the same material displays flow textures such as pinch-and-swell structures, folds and shear bands. We interpret these structures as representing the deformation and subsequent crystallization stage of a gelling, silica oversaturated, viscous fluid.

Material studied was sampled from the Sanddøla fault in Norway, which is a late Caledonian structure occurring at the northern rim of the Grong basement culmination in the central Scandinavian Caledonides (Stel 1988). The fault is part of the late Caledonian fault system of Western Europe (Ziegler 1990), which includes the Great Glen fault and the Trondheim fjord lineaments (Grønlie & Roberts 1989). There is evidence that the Sanddøla fault originated by wrenching and was reactivated by a dip-slip movement (Stel 1988). The fault occurs in leucocratic gneisses and is characterized by extensive hydrothermal veining of quartz, chlorite, prehnite and chalcedony. Movement along the fault is characterized by repetitive alternation of ductile and brittle episodes. The latest brittle structures however, are not overprinted by subsequent ductile deformation.

MICROSTRUCTURES

The cataclasites contain pink-coloured ultra-fine-grained veins made up of feldspar clasts embedded in cryptocrystalline silica. The veins transect earlier foliations and are associated with offset of the vein walls. The feldspar clasts are very irregularly shaped with rough, rupture-type boundaries, and are clearly crush frag-

ments (Fig. 1). Commonly a foliation is defined by alignment of inequant clasts, which is associated with an alternation of clast-rich and poor bands. The origin and aspect of microstructure is divergent on the micrometre and millimetre–centimetre scale, as described below.

Texture of foliated veins

Polished rock slices were used to study the centimetre-scale structure of the foliation in the veins. The relatively high translucency of the silica reveals the three-dimensional packing structure of the crush fragments, which is essential to observe foliation. It is not revealed in ordinary thin sections which only show a two-dimensional section through the larger clasts. Three types of veins are distinguished on the basis of micro-structures: type (1)–(3).

Type (1) veins demonstrate a repetitive variation in the amount and size of feldspar clasts (Fig. 1a), defining a planar banding that extends from one vein wall to the other. There is no fixed orientation relationship between type (1) banding and the vein wall. Locally, the layering appears to vanish as it is transitional to a zone of chaotic texture in which silica carries a non-sorted clast load. A similar texture is found in 'shoot-off' injection veins (Fig. 1a), which bear strong similarities to liquidized sand injection veins in unconsolidated sediments. Locally, an agate type of banding is found, defined by a regularly spaced variation in hematite precipitates (Fig. 1b). Locally, these layers are broken up and are enclosed by microveins of coarse-grained quartz. These microveins are restricted to microcrystalline domains only, and do not persist in the vein wall.

Type (2) veins show a pronounced grading with a decrease in clast size from one vein wall to the other (Fig. 1c). The finest grained parts grade into zones of inclusion-free silica. The largest clasts (*ca* 1 mm) are randomly oriented and display no foliation. In domains where the clast size is smaller, a foliation is defined by bands with variable clast content Type (2) veins display microstructures which are indicative of flow, such as pinch-and-swell structure, micro-boudinage and folds (Figs. 1c & e). Some micro-boudinage resulted in rupture of the layering, while the foliation in the matrix pinches out in a similar way as in brittle–ductile foliation boudinage (Platt & Vissers 1980). Characteristically, layers that contain the largest amount of clasts are boudinaged, while relatively clast-poor layers are wrapped around the microboudins. There is a progressive grading from clast-free cryptocrystalline material to a zone of larger, idiomorphic quartz crystals (Figs. 1c & d). These crystals occur in structures which have been described as 'radiate bladed' (Sweetman & Tromp 1991). This structure is characterized by a 0.1 mm thick blade of cryptocrystalline quartz on which idiomorphic crystals of approximately 1 mm in size are found. *c*-axes of the crystals point away from the central blades. The blades constitute three-dimensional networks, and have no intervening matrix. These structures are thought to be diagnostic of a specific crystallization mechanism which is discussed in detail in a later section.

Type (3) veins display a foliation which is asymmetrical with respect to the vein walls (Fig. 1f). Characteristically, a sigmoidal pattern occurs with a foliation oriented at 30–45° to the vein wall in the centre that consistently rotated towards parallelism near the vein walls. It is locally wrapped around larger clasts and displays asymmetric micro-boudinage and pinch-and-swell structures. Type (3) veins also show a stratification with respect to size and relative amount of crush fragments. In the core of the veins largest clasts are found while near the vein walls extremely fine-grained (0.1 μm), dust-sized inclusions occur. Cross-cutting relations between different type (3) veins are found, in which the foliation on one vein is clearly truncated by another.

Structure of cryptocrystalline silica

The micro- and substructure of cryptocrystalline silica was revealed by optical microscopy, cathodoluminescence and transmission electron microscopy (TEM), and has been largely described before in Stel (1981). Additionally, SEM analyses were performed on polished sections; this technique bridged the observations by optical microscopy and TEM.

In optical microscopy the fine-grained clast-bearing silica matrix is observed to have a transitional relationship to spherulitic, feather-type chalcedony and to idiomorphic quartz crystals (Fig. 2). TEM demonstrated banding in crystallites by preferential electron-beam-induced damaging patterns along growth planes parallel to crystal faces. This substructure is interpreted to be diagnostic for neo-crystalline phases, and has never been encountered in deformed crystals. Cathodolumi-

Fig. 1. (a)–(d). Micrographs of polished sections (incident light) of microveins in cataclasites. Microveins consist of cryptocrystalline silica and are loaded with feldspar crush fragments. Crush fragments usually demonstrate layering and stratification, characterized by variations in the amount and size of crush fragments. (a) Type (1) vein, demonstrating a planar layering (S-s), which is continuous from one vein wall to the other. Locally, the layering 'disappears' and non-sorted non-packed veins occur in shoot-off structures, which are interpreted as injection veins (I). Scale bar: 2 mm. (b) Type (1) vein, filled with comb quartz (translucent) and chalcedony (milky). Note Liesegang-bands (L) (rhythmic banding of hematite rich zones) parallel to the vein wall. At S, Liesegang bands are disruptive and micro-brecciated. Fragments are enclosed by comb-quartz rich veins, interpreted as shrinkage cracks (see Fig. 4). Scale bar: 1 mm. (c) 'Graded bedding' in type (2) veins, with large crush fragments in chaotic texture in the lower part, and gradually finer grained crush fragments towards the top of the vein. The latter are transitional to clast-free domains, which in turn grade into coarse-grained, euhedral quartz in plate structures (P). Fine-grained fragments demonstrate layering by variation in size of crush fragments. Note pinch-and-swell structures, which are indicative for flow in ductile material containing viscosity contrasts. Scale bar: 1 mm. (d) Folds and boudins (B) in coarse-grained part of a type (2) vein, illustrating the effect of amount of dispersed particles on viscosity. Scale bar: 1 mm.

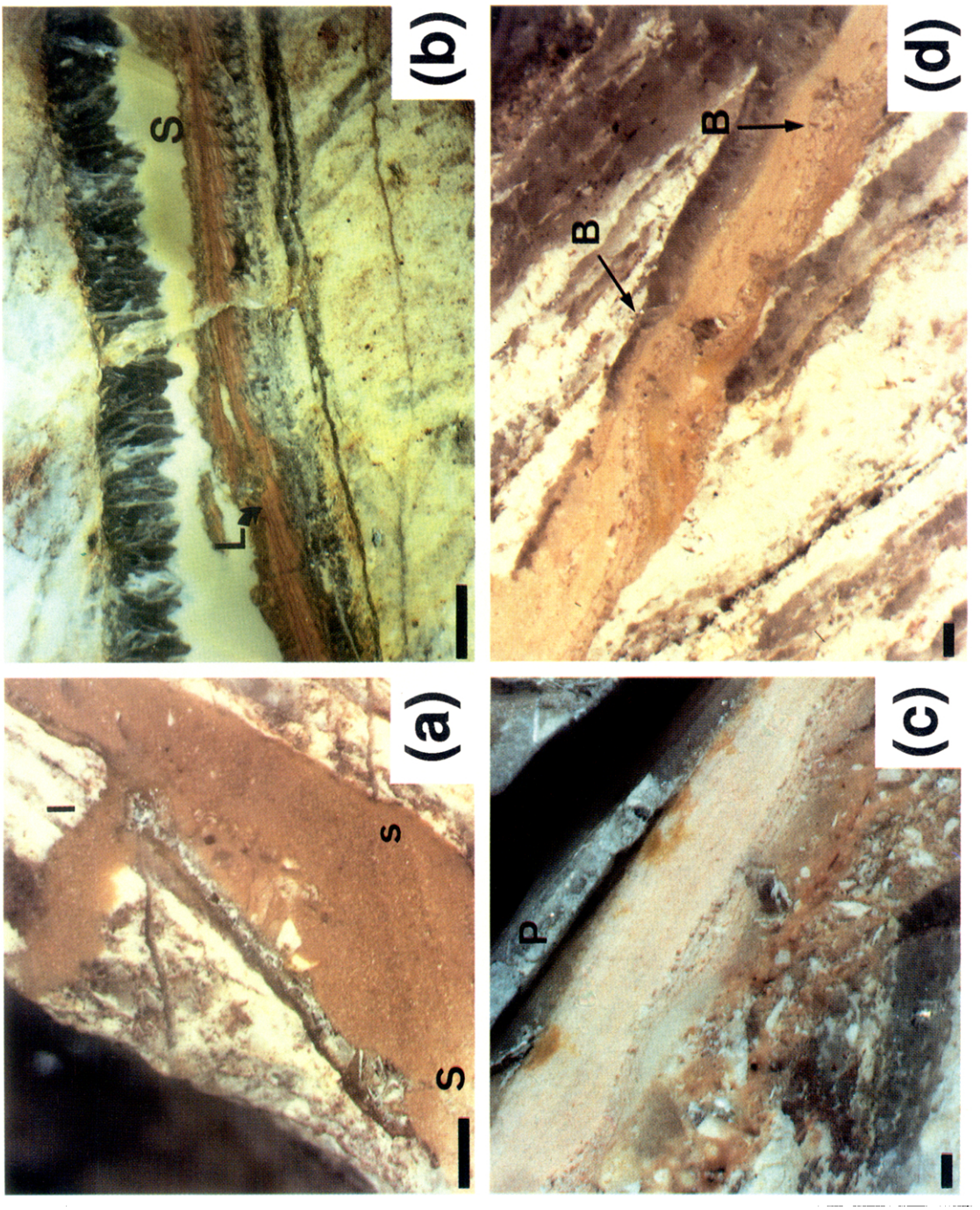
(b)
S
(d)
B
B
(a)
I
S
S
(c)
P

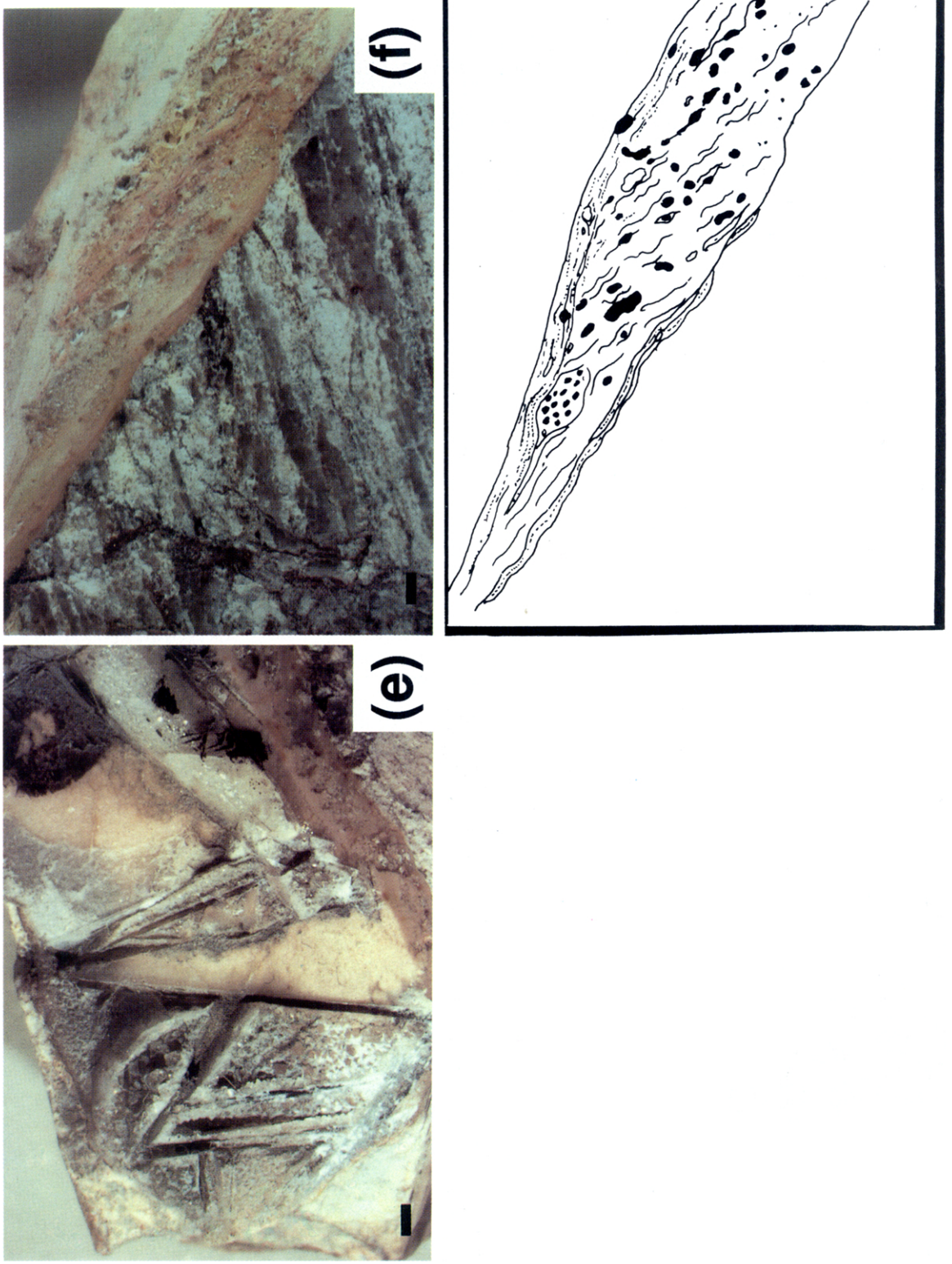

Fig. 1. (e) Radiate blade quartz that occur at the top of type (2) veins. Euhedral quartz crystals occur on plates that constitute three-dimensional networks, interpreted as shrinkage cracks in silica gel (see Fig. 5 for an interpretive cartoon). Scale bar: 1 mm. (f) Micrograph and line drawing (below) of type (3) vein, showing monoclinic symmetry of fabric in clast-loaded cryptocrystalline silica vein. This type of vein is interpreted as a sheared type (1) vein. Scale bar: 1 mm.

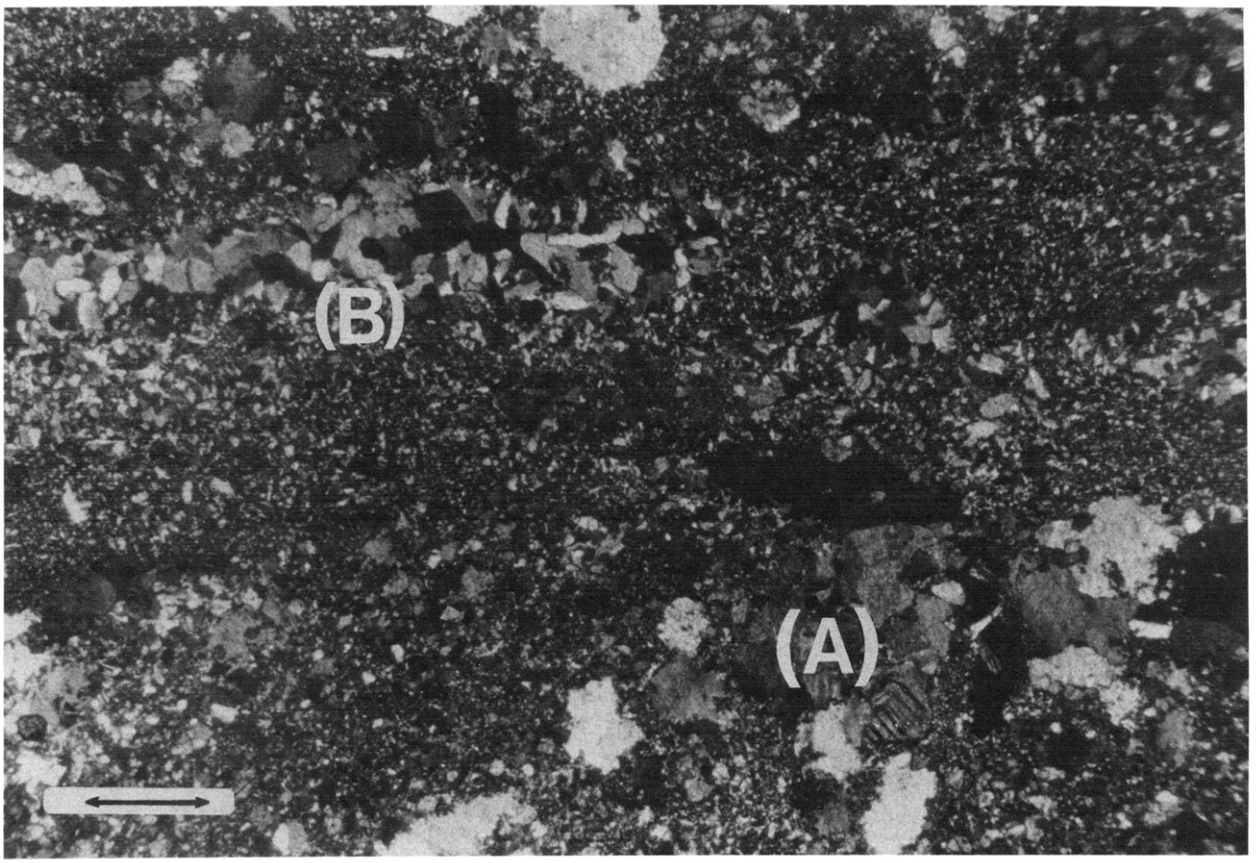

Fig. 2. Micrograph (crossed polarizers) showing a typical example of the microstructure of a cataclasite from the Sanddøla fault. At the bottom right, a rock fragment is visible (A) which 'floats' in a fine-grained matrix of chalcedony and feldspar crush-fragments. This matrix has transitional relations to coarse-grained quartz crystals showing euhedral boundaries (B). Scale bar: 1 mm.

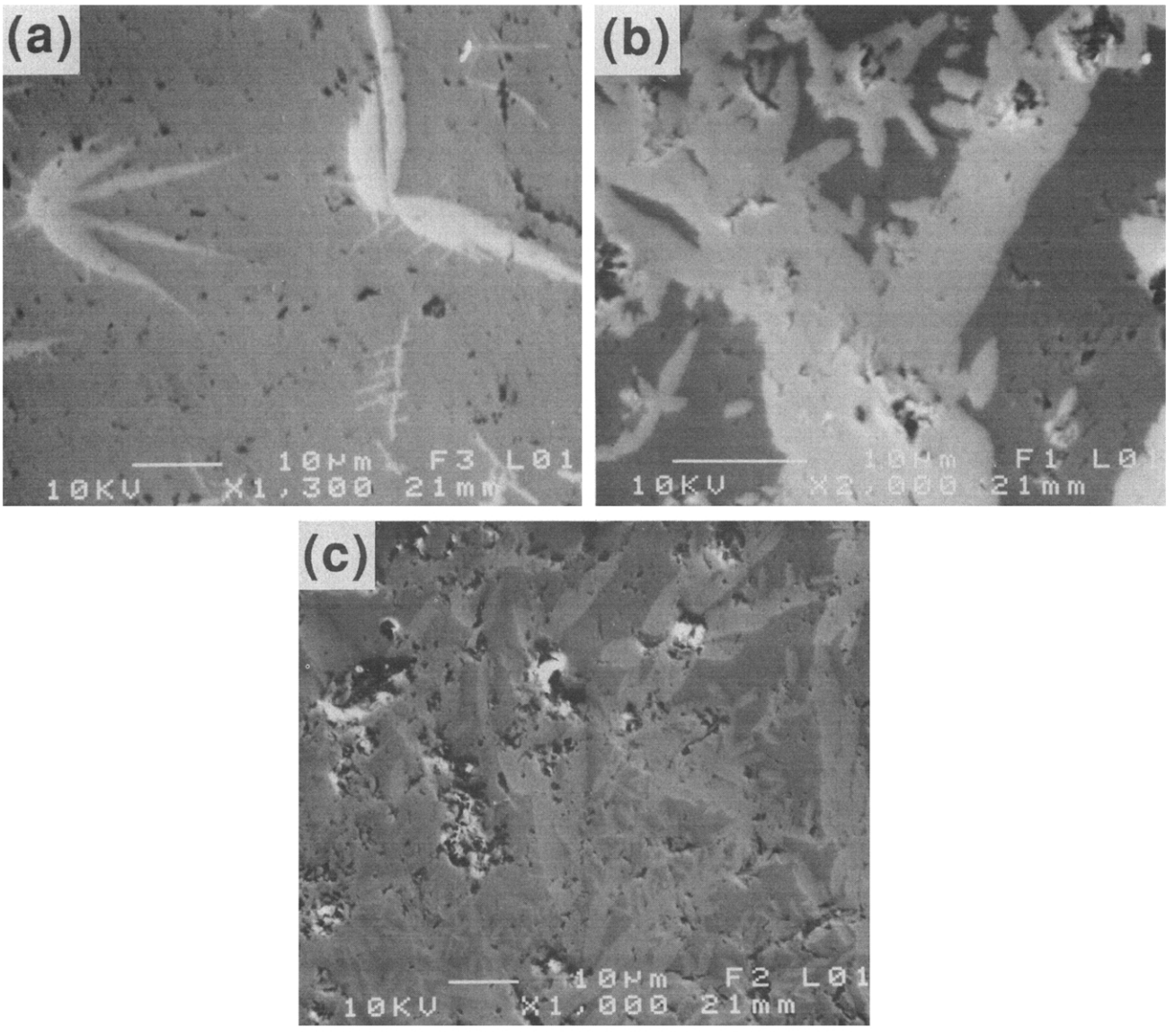

Fig. 3. SEM photographs (backscatter detector) of the substructure of cryptocrystalline silica. (a) Quartz crystallites (white) in a dark-coloured, porous matrix. Colour difference is due to density contrast. Both crystallites and matrix are silica phases. (b) Sheaf-like clusters of quartz crystallites in opaline matrix. Note the occurrence of crush fragments in the centre of individual sheafs. (c) Overview of network formed by quartz crystallites.

nescence revealed an agate type structure in the gouge that encompasses thousands of crystallites, suggestive of a pre-crystallization structure of the material.

Polished and carbon-coated sections of cryptocrystalline aggregates were studied with a scanning electron microscope (SEM) coupled to an energy dispersive X-ray analytical system. Observations were performed using a backscattered electron detector by which image contrast reflects the variation in density. This technique revealed the occurrence of relatively dense crystallites of approximately 10 μm in a uniform, dark-coloured porous matrix (Fig. 3a). The spherulites and sheaf-like clusters constitute networks of randomly oriented crystals (Fig. 3b). Individual sheafs appear to radiate from a central point at which a feldspar clast is located. Both dense crystallites as well as the matrix emitted X-rays with energy levels unique for Si. Thus it was established that the matrix is a silica phase with a density lower than that of quartz. These observations suggest that the cryptocrystalline aggregates are composed of quartz crystallites in a matrix of chalcedony. The lower density of the latter (approximately 1% lower than that of quartz would explain the observed SEM contrast.

Fluid inclusions

Quartz crystals contain liquid–vapour (LV) type fluid inclusions with rounded or near negative crystal shape, which occur as isolated inclusions as well as in trials which were probably trapped in healed microcracks. The inclusions were studied using a heating–freezing stage. By this method, the melting temperature T_m of the liquid phase and the liquid–vapour homogenization temperature T_h of the LV inclusions were established. Melting temperatures of the trapped fluid ranges from -6.8 to -0.1°C, indicating a NaCl-equivalent wt% of 10–0.4 (Zang & Frantz 1987). Homogenization temperatures of the liquid–vapour inclusions range from 140 to 180°C, with the highest frequency in the range of 150–160°C. No significant difference between isolated LV inclusions and those found in trails were found.

One group of fluid inclusions was found which consist of pure water with a T_m of 0°C, and contain no vapour phase. The trail in which these inclusions are found overprints all the other trails and is considered to represent the latest generation of healed cracks.

INTERPRETATION

Clast-loaded cryptocrystalline silica veins demonstrate pinch-and-swell structures, boudins, folds and boudinaged folds, as well as shear-band structures on centimetre scale. This association of microstructures provides strong evidence for ductile flow. On the micrometre scale however, the same material demonstrates a crystallization texture that is characterized by spherulitic and sheaf-like clusters of quartz crystallites in a chalcedonic matrix. Apparently, crush fragments acted as the nuclei for the crystallites while in the absence of fragments, less dense opaline-like substances precipitated. Such a texture can be created by rapid crystallization from oversaturated fluids (Flörke *et al.* 1990). The crystallites are demonstrably undeformed as shown by TEM (Stel 1981). This is confirmed by SEM observations that reveal a delicate pattern of thin, undeformed dendritic intergrowths. We therefore conclude that the observed deformation and flow structures were formed in a pre-crystallization stage. Such a phase could not have been a silica melt, included feldspar fragments would then have reacted to form a cotectic phase. *A priori*, there are three alternative types of fluid from which crystallization could have taken place: an oversaturated true solution, a silica sol, or a (hydro)silica gel (Keith & Padden 1962, Langer & Flörke 1974, Oehler 1976, Yariv & Cross 1979, Flörke *et al.* 1990, Sweetman & Tromp 1991, Harder 1993). These types of fluids can be transitional to each other, and differ basically in the degree of polymerization. Polymerized silica can be expressed by the following formula:

$$Si_nO_{2n-m}(OH)_{2m}. \quad (1)$$

Silica polymers are in solution when $n < 6$, and in dispersion when $n > 6$ (Yariv & Cross 1979). A gel structure develops when the silica particles constitute a three-dimensional network (Iler 1979, p. 222). Although we have no direct evidence for the nature of the fluid, the microstructures of the veins allow a qualitative reconstruction of its physical properties such as described below. On this basis, we propose that the fluid in which the silica minerals crystallized was a viscous silica-oversaturated sol, or a silica hydrogel.

Sedimentation and flow textures

The microstructure of the veins allows a qualitative determination of the viscosity of the presumed fluid phase. The stratification in type (1) and (2) veins is interpreted as a settling structures. In type (2) veins there is a clear grading in size of clasts from bottom to the top. The coarsest grains have a packing (clast-supported) texture and show no foliation, while finer grained parts display lamination. The pattern is strongly similar to sedimentary structures in re-settled liquidized sediments (Postma *et al.* 1983), while comparable structures are formed by crystal settling in convecting magmas (Sparks *et al.* 1993). We interpret this structure accordingly, as resulting from the settling of dispersed particles in a flowing viscous fluid. However, only the larger crush fragments settled during sedimentation. In offshoots from type (1) veins, no grading of crush fragments is visible, and the particles are non-packed as they 'float' in a cryptocrystalline matrix (Fig. 1a). Likewise, smaller clasts (<1 mm) in type (2) veins do not show a packing structure and are 'matrix-supported'. They are concentrated in the lower half of the vein, suggesting that settling was obstructed and that particles were 'frozen-in' during solidification. To explain the apparent obstruction of particle settling, we propose that the viscosity of the fluid increased. The viscosity of a

polymerizing fluid increases when the volume fraction of dispersed particles increases (Einstein 1905, Frankel & Acrivos 1967) and its flow behaviour eventually changes from Newtonian to Bingham plastic (Ide & White 1974, Kalyon *et al.* 1993). The settling of small particles is obstructed if their apparent weight per unit area is smaller than the yield stress. In this way the spatial distribution of particles in a fluid can be fixed, and flow, as well as settling structures are frozen in.

Apparently, the presently described structures were generated in a fluid of which the viscosity was low enough to allow flow folding, but gradually increased to a value that was high enough to preserve the flow instabilities. A comparable condition is thought to control the generation and preservation of flow folds in cooling pyroclastic flows. Such structures are preserved when the viscosity ranges from 10^4 to 10^6 Poise (Fisher & Schmincke, 1984, pp. 214–218) and we therefore suggest that the viscosity of the fluid in the veins was comparable to that value.

Crystallization textures

Using SEM, cryptocrystalline silica domains displays a texture that is characterized by spherulitic and sheaf-like clusters of quartz crystallites of approximately 10 μm long with near euhedral outlines (Fig. 3). The presence of feldspar fragments in the centres of the sheaf-like clusters strongly suggests that these acted as crystallization nuclei. The crystallites appear to 'float' in the matrix and show no preferred shape orientation. This suggests that crystal growth took place in a highly viscous medium that prevented sedimentation. In the absence of feldspar fragments agate-banded chalcedony formed, which probably has an amorphous, gel-like precursor (Harder 1993). It is interpreted that the banding originated as Liesegang bands in the gel phase (Henish 1988). The texture of the silica minerals is compatible to that of experimentally produced textures, produced either by devitrification (Liu *et al.* 1992) or by crystallization of a gel (Luan & Paterson 1992). In both cases seed crystals act as nucleation centres for crystal growth in a viscous medium by which spherulitic structures are generated (Liu *et al.* 1992).

There are two types of microstructures which suggest that during crystallization, shrinkage took place: brecciation of agate-type layered cryptocrystalline domains and the occurrence of radiate blade quartz. As illustrated by Fig. 1(b), locally an agate-type of layering is found in cryptocrystalline domains. This layering is disrupted by wedge-shaped veins, that taper out against the vein wall. Apparently, these veinlets did not form by extension as wedge-shaped extension gashes should be associated with rotation of the fragments. Instead, the internal layering of each fragment retained its parallelism to the vein wall. We therefore propose that the veins represent shrinkage cracks. Oehler (1976) suggested a mechanism to explain these type of shrinkage cracks during crystallization of silica gel. He considered that solidification of a silica gel takes place by polymerization of $Si_nO_m(OH)_{2n-m}$ groups in the fluid and a volume decrease takes place during which the released water is expelled from the gel. The process is illustrated by Fig. 4. It is envisaged that by shrinkage of banded gel upon crystallization, a water-filled network of cracks is formed (Fig. 4b), in which at a later stage crystallization of quartz may take place (Fig. 4c) either as vein quartz or as idiomorphic crystals in free space (Fig. 4c). Sweetman & Tromp (1991) interpreted the texture of 'radiate bladed' quartz and suggested that upon cooling of a silica gel, shrinkage cracks are formed and a true solution is separated from the gel (Figs. 5a&b). The fluid migrates into the cracks, in which cryptocrystalline quartz precipitates and constitute planar 'blades' which mimic the shape of the cracks (Fig. 5c). These 'blades' subsequently serve as the substratum on which euhedral crystal growth takes place by dissolution–crystallization reaction at the expense of the amorphous silica particles in the intervening gel. Eventually, the gel has been dissolved completely, leaving a network of intersecting cryptocrystalline blades and euhedral quartz crystals (Fig. 5d).

In conclusion, there is microstructural evidence indicative for the presence of a high viscous fluid in which flow structures are preserved. Apparently, during crystallization, shrinkage of this phase took place in a similar way as in crystallizing gels; while the crystallization textures are compatible with those which are known to occur in gels. We therefore conclude that the fluid from which crystallization took place was a silica-hydrogel.

The texture of the three types of foliated veins can now be readily interpreted as due to flow, injection and deformation of a clast-loaded viscous fluid. Pinch-and-swell structures and microboudinage, as well as folds are due to deformation of material with layered viscosity contrasts. It can readily be appreciated that those parts of the vein with the highest clast density correlate with highest viscosity, as they were preferentially 'broke-up' (cf. Ottino 1989, pp. 300–307). The foliation in type (1) veins is interpreted as due to settling of fragments in a fluid at rest. Offshoots from type (1) veins demonstrate a random texture and carry an unsorted clast load. The structure is similar to that of injected, liquidized veins (Allen 1982) and is interpreted accordingly. Type (2) veins are interpreted as 'frozen-in' flow structures of a clast-loaded fluid, developing a mass-flow type of texture. Type (3) veins are interpreted as sheared veins, demonstrating a pseudo-monoclinic fabric symmetry with respect to the vein walls. This is supported by the occurrence of similar folds and asymmetric wrap structures of foliation around larger clasts.

Temperature constraints

The silica veins described above are associated with prehnite veins. This gives an upper limit for the temperature of formation of 400°C (Liou *et al.* 1983). A lower limit of the temperature at which the bulk of the fluid inclusions in quartz have been trapped is given by the homogenization temperature of the water–vapour in-

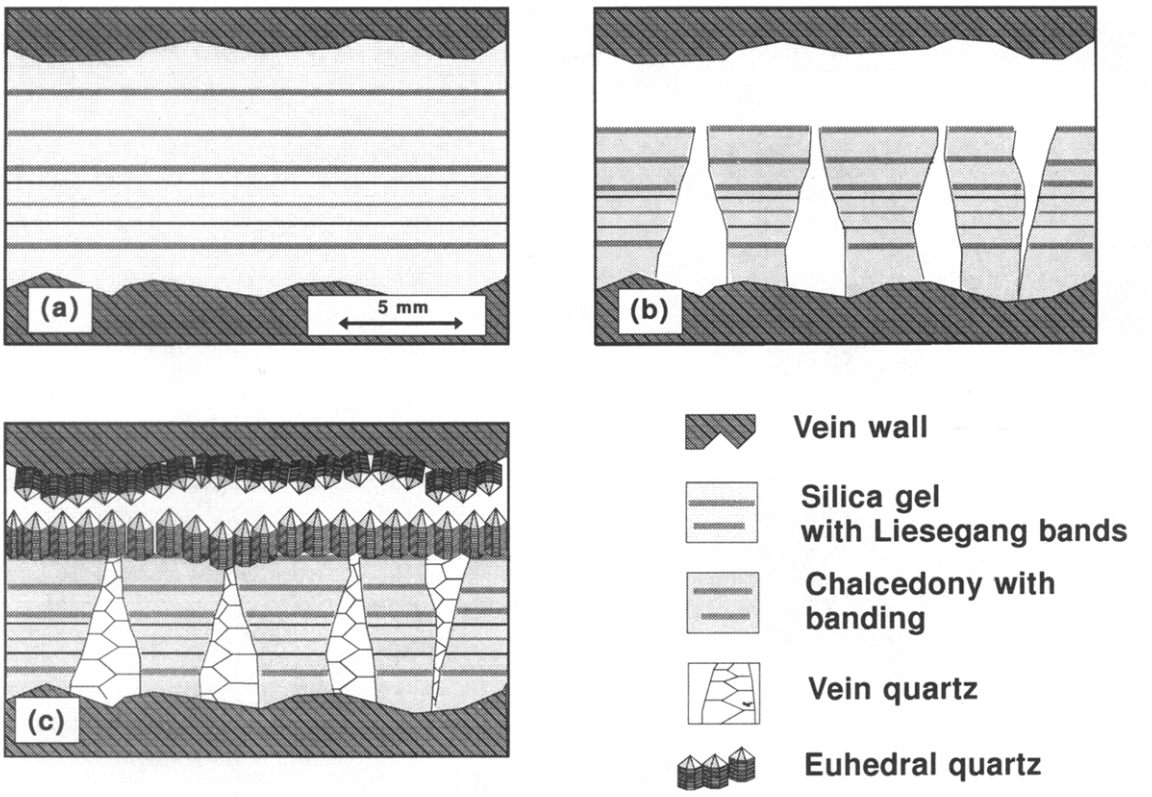

Fig. 4. Cartoon illustrating the formation of shrinkage cracks during crystallization of a silica gel (cf. Oehler 1976). (a) Stage (1), showing an extension vein filled with banded silica gel. The banding is defined by periodic variation in amount of haematite, interpreted as Liesegang bands. (b) Stage (2), upon crystallization of the gel shrinkage takes place and a system of fluid-filled cavities is created. (c) Stage (3), in fluid-filled cavities crystallization of quartz takes place.

clusion in the quartz, which is 150–160°C (Zang & Frantz 1987). As the minerals have grown in hydrothermal veins, probably in a cooling fluid, this temperature range gives no information of the depth at which these processes have taken place. The trail of fluid inclusions which contain no vapor phase, and has a melting point of 0°C must have been trapped at a temperature ≤100°C (Zang & Frantz 1987). If this represents the final cooling temperature of the hydrothermal fluid, corresponding to the temperature of country rock, the depth of the exposed fault section would be lower than 3 km assuming a geotherm of 33°C km^{-1}. The time relation of these inclusions to the crystallization of the quartz is however unknown, as it is well possible that the inclusions were trapped at a much later stage.

Formation of gel in cataclasites: a model

The presence of cryptocrystalline silica strongly suggests that the fluid in which crystallization took place was highly silica-oversaturated (Flörke *et al.* 1990). Experimentally, such fluids can be generated by quenching a hot fluid against a cold vein wall. Similar processes take place in geothermal vents, where silica gels occur in various state of dehydration, from water-rich gelatinous to glass-like material (Lebedev 1967, Czernichowski-Lauriol & Fouillac 1991). We propose that cryptocrystalline silica in cataclasites described here has a similar origin: quenching of a hydrothermal fluid that migrated through a fault zone (Sibson 1987, 1989). Harder (1993) reports that oversaturation alone can cause formation of a dilute gel. However, it is envisaged that in the present case gel formation was enhanced by admixture of colloidal silica particles. Recent work on experimental brittle faulting of siliceous rocks shows that by grinding amorphization of minerals (specifically quartz) takes place by growth of amorphous silica at planar defects (Yund *et al.* 1990, Winters *et al.* 1992, Kingma *et al.* 1993). This result confirms earlier interpretations that amorphous silica in fault zones as a consequence of communication during cataclasis (Wenk 1978, Yariv & Cross 1979). In the laboratory, silica gel has been produced simply by mechanical mixing of silica solution with crush fragments of amorphous silica (Iler 1979, p. 438). Wilkinson *et al.* (1993) reported the occurrence of silica-gel 'fluid inclusions' in crack annealing experiments by quenching a hot mixture of powdered quartz and an alkaline solution. We propose that a similar process has taken place in the presently discussed case.

DISCUSSION AND CONCLUSIONS

Microstructures indicate that during deformation, a viscous, silica oversaturated fluid was present in cataclasites from the Sanddøla fault. There are indications that the formation of gel, or at least amorphous silica is also common in other fault zones. Chalcedony and jaspis-filled veins have been observed in other low grade faults as well, for example in steep dip-slip faults in the Svecofennian orogen of SW Finland (Stel *et al.* in press).

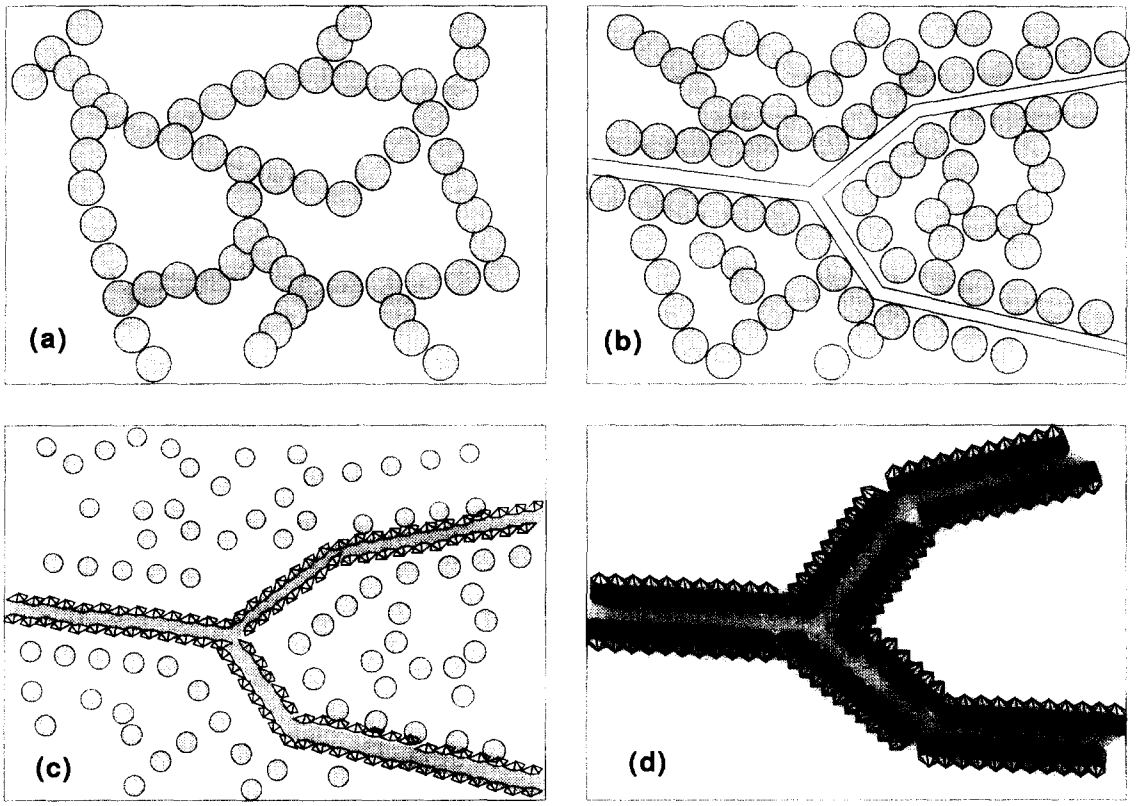

Fig. 5. Cartoon illustrating the formation of 'radiate blade quartz' after Sweetman & Tromp (1991). The cartoons are not to scale; the size of the silica particles in (a), (b) and (c) is approximately 100 Å, while the width of the cryptocrystalline 'blades' is approximately 0.1–0.5 mm. (a) Starting material: a silica gel which is composed of amorphous particles (dotted) in a solution. (b) By cooling, shrinkage cracks are formed. (c) By a solution–precipitation reaction, the amorphous silica dissolves and euhedral quartz crystals nucleate on the cryptocrystalline blades. (d) Growth of the crystallites takes place at the expense of gel until the latter has been dissolved completely, leaving the radiate blade quartz texture, characterized by 'blades' of cryptocrystalline quartz loaded with euhedral quartz crystals in free space.

Sweetman & Tromp (1991) suggest that the above described radiate blade quartz structure was formed from silica gels in basement faults in Zimbabwe. In addition, ultrafine-grained quartz occurs on fault slickensides, such as described by Power & Tullis (1989). These authors suggested that precipitation from a colloidal fluid is a possible mechanism of formation of these structures.

Presence of a gel in a fault may have important consequences for the interpretation of fault-rock history. A viscous gel will reduce the shear strength of a fault zone to practically zero, and enable non-seismic slip. However, since crystallization proceeds rapidly, a non-seismic slip event will be short-lived. Microstructures demonstrate that crystallization products of silica gels are ubiquitous in microcracks, indicating that fault rocks are completely healed. After such a pervasive healing stage a massive, chert-like rock has been formed, which is free of microcracks, and thus it has a considerable strength. Crystallization and restoration of fault rock cohesion will allow reaccumulation stress, which eventually may lead to a new phase of brittle failure. The periodicity of seismic events in the Earth's crust may depend not only on the rate by which stress is built up, but also on the rate of fault-rock restoration. Silica gels may crystallize instantaneously, for instance when the pH value is changed upon mixing with other fluids. Crystallization of gels may take place within minutes, hours or years, or it may remain a viscous substance, depending on the physical and chemical environment (Henish 1988). Consequently, its behaviour must be considered as one of the factors determining the periodicity of seismic stress release in the Earth's crust.

In conclusion, there is evidence for the presence of a viscous, silica oversaturated fluid in cataclasites. This fluid carried feldspar crush fragments, varying in size from 0.1 μm to 2 mm. In some cases, clasts were settled, yielding sedimentary fabrics such as graded bedding. Settling of clasts was far from completed, and smaller clasts did not settle due to increasing viscosity, which is interpreted as due to polymerization of O–Si–O networks that eventually caused precipitation of solid silica. Clast-loaded veins show deformation textures indicative for flow, while the silica matrix is demonstrably undeformed. This indicates the syn-kinematic presence of the viscous fluid. There is strong microstructural indication that in a late stage the fluid was a hydrogel, which upon dehydration and associated shrinkage crystallized as radiate blade quartz.

Acknowledgements—SEM microscopy was performed by Saskia Kars from the micro-analytical laboratory of the Vrije Universiteit. Professor Dr O. W. Flörke, Professor Dr P. Hartman and an anonymous reviewer have made many valuable suggestions to improve this manuscript.

REFERENCES

Allen, J. R. 1982. *Sedimentary Structures*. Elsevier, Amsterdam.

Babaie, H. A., Babaie, A. & Hadizadek, J. 1991. Initiation of cataclastic flow and development of cataclastic foliation in nonporous quartzites from a natural fault zone. *Tectonophysics* **200**, 67–77.

Chester, F. M. & Higgs, N. G. 1992. Multimechanism friction constitutive model for ultrafine quartz gouge at hypocentral conditions. *J. geophys. Res.* **97**, 1859–1870.

Chester, F. M., Evans, J. P. & Biegel, R. L. 1993. Internal structure and weakening mechanisms of the San Andreas fault. *J. geophys. Res.* **98**, 771–786.

Czernichowski-Lauriol, I. & Fouillac, C. 1991. The chemistry of geothermal waters: its effect on exploitation. *Terra Nova* **3**, 477–492.

Dieterich, J. H. & Conrad, G. 1984. Effect of humidity on time and velocity dependent friction in rocks. *J. geophys. Res.* **89**, 4196–4202.

Einstein, A. 1905. Uber die von molekularkinetischen Theorie der Wärme geforderte Bewegung von in ruhenden. Flüssigkeiten suspendierten Teilchen. *Ann. Physik* **17**, 549.

Engelder, J. T., Logan, M. & Handin, J. 1975. The sliding characteristics of sandstone on quartz gouge. *Pure & Appl. Geophys.* **113**, 68–86.

Fisher, R. V. & Schmincke, H. U. 1984. *Pyroclastic Rocks*. Springer, Berlin.

Flörke, O. W., Graetsch, H. & Jones, J. B. 1990. Hydrothermal deposition of cristobalite. *Neues Jb. Miner. Mh.* **1990**, 81–95.

Frankel, N. A. & Acrivos, A. 1967. The viscosity of a concentrated suspension of solid spheres. *Chem. Engng Sci.* **22**, 847–853.

Grønlie, A. & Roberts, D. 1989. Resurgent strike slip duplex development along the Hitra-Snåsa and Verran faults, Møre-Trøndelag fault zone, central Norway. *J. Struct. Geol.* **11**, 209–305.

Harder, H. 1993. Agates formation as a multicomponent colloid chemical precipitation at low temperatures. *Neues Jb. Min. Monatsh.* **1**, 31–48.

Henish, C. 1988. *Crystallization From Gel and Liesegang Rings*. Cambridge University Press, Cambridge.

Ide, Y. & White, J. L. 1974. Rheological phenomena in polymerization reactions rheological properties, and flow patterns around agitates in polystyrene–styrene solution. *J. Appl. Polym. Sci.* **18**, 2997–3018.

Iler, R. K. 1979. *The Chemistry of Silica: Solubility, Polymerization, Colloid and Surface Properties and Biochemistry*. Wiley, New York.

Kalyon, D. M., Yaras, P., Aral, B. & Yilmazer, U. 1993. Rheological behavior of a concentrated suspension- A solid rocket fuel simulant. *J. Rheol.* **37**, 35–53.

Keith, H. D. & Padden, F. J. 1962. A phenomological theory of spherulite crystallization. *J. Appl. Phys.* **34**, 2409–2421.

Kingma, K. J., Meade, C., Hemley, R. J., Mao, H. K. & Vebleu, D. R. 1993. Microstructural observations of alpha-quartz amorphization. *Science* **259**, 666–669.

Langer, K. & Flörke, O. W. 1974. Near infrared absorption spectra of opals and the role of water in these minerals. *Fortschr. Miner.* **52**, 17–51.

Lebedev, L. M. 1967. *Metacolloids in Endogenic Deposits*. Plenum Press, New York.

Liou, J. G., Kim, H. S. & Maruyma, S. 1983. Prehnite–epidote equilibria and their petrologic application. *J. Petrol.* **24**, 321–342.

Liu, C. L., Komarneni, S. & Roy, S. 1992. Crystallization of anorthite seeded albite glass by solid state epitaxy. *J. Am. Ceram. Soc.* **75**, 2665–2670.

Luan, F. C. & Paterson, M. S. 1992. Preparation and deformation of synthetic aggregates of quartz. *J. geophys. Res.* **97**, 301–320.

Oehler, J. H. 1976. Hydrothermal crystallization of silica gel. *Bull. geol. Soc. Am.* **87**, 1143–1152.

Ottino, J. M. 1989. *The Kinematics of Mixing: Stretching, Chaos and Transport*. Cambridge University Press, Cambridge.

Platt, J. P. & Vissers, R. L. M. 1980. Extensional structures in anisotropic rocks. *J. Struct. Geol.* **2**, 397–410.

Power, W. L. & Tullis, T. E. 1989. The relationship between slickenside surfaces in fine grained quartz and the seismic cycle. *J. Struct. Geol.* **11**, 879–893.

Postma, G., Roep, Th. B. & Ruegg, G. H. J. 1983. Sandy-gravelly mass low deposits in an ice-marginal lake, with emphasis on plug-flow deposits. *Sedim. Geol.* **34**, 59–83.

Rutter, E. H. & Maddock, R. H. 1992. On the mechanical properties of synthetic kaolinitic quartz fault gouge. *Terra Nova* **4**, 489–500.

Rutter, E. H., Weddoch, S., Hall, S. H. & White, S. H. 1986. Comparative microstructures of natural and experimentally produced clay-bearing fault gouges. *Pure & Appl. Geophys.* **124**, 3–30.

Rutter, E. H. & White, S. H. 1979. The microstructure and rheology of fault gouges produced experimentally under wet and dry conditions at temperatures up to 400°C. *Bull. Minéral* **102**, 101–109.

Sibson, R. H. 1987. Earthquake rupturing as a hydrothermal mineralizing agent. *Geology* **15**, 701–704.

Sibson, R. H. 1989. Earthquake faulting as a structural process. *J. Struct. Geol.* **7**, 503–600.

Sparks, R. S., Huppert, H. E., Koyaguchi, T. & Hallworth, M. A. 1993. Origin of modal and rhytmic igneous layering by sedimentation in a convecting magma chamber. *Nature* **361**, 246–249.

Stel, H. 1981. Crystal growth in cataclasites: diagnostic microstructures and implications. *Tectonophysics* **78**, 585–600.

Stel, H. 1988. Basement–cover relations at the Grong–Olden culmination, central Norway. *Norsk geol. Tidsskr.* **68**, 135–147.

Stel, H., Cloetingh, S., Heeremans, M. & van der Beek, P. In press. Anorogenic granites, magmatic underplanting and the origin of intracratonic basins in a non-extensional setting. *Tectonophysics*.

Sweetman, T. M. & Tromp, P. L. 1991. Radiate bladed quartz from Zimbabwe. *Mineralog. Mag.* **55**, 138–140.

Wenk, H.-R. 1978. Are pseudotachylites products of fracture or fusion? *Geology* **6**, 507–511.

Yariv, S. & Cross, H. 1979. *Geochemistry of Colloid Systems*. Springer, Berlin.

Wilkinson, J. J., Rankin, A. H. & Nolan, J. 1993. Aqueous-silica immiscibility in the system K_2O–CO_2–H_2O–SiO_2. (Abs.) *Terra Nova* **5**, Abs. Suppl. 1, 441.

Winters, R. R., Garg, A. & Hammack, W. S. 1992. High-resolution transmission electron microscopy of pressure-amorphized alpha-quartz. *Phys. Rev. Lett.* **69**, 3751–3753.

Yund, R. A., Blanpied, M. L., Tullis, T. E. & Weeks, J. D. 1990. Amorphous material in high strain experimental fault gouges. *J. geophys. Res.* **95**, 15,589–15,602.

Zang, Y. G. & Frantz, J. D. 1987. Determination of the homogenization temperatures and densities of supercritical fluids in the system. NaCl–KCl–$CaCl_2$–H_2O using synthetic fluid inclusions. *Chem. Geol.* **64**, 335–350.

Ziegler, P. A. 1990. *Geological Atlas of Western and Central Europe*. Geol. Soc. Publishing House, Avon.

Zoback, M. D., Zoback, M. L., Mount, V. S., Suppe, J., Eaton, J. P., Healy, J. H., Oppenheimer, D., Reasenberg, P., Jones, L., Raleigh, C. B., Wong, I. G., Scotti, O. & Wentworth, C. 1987. New evidence on the state of stress of the San Andreas fault system. *Science* **238**, 1105–1111.